Research Article

High-power, narrow linewidth solid-state deep ultraviolet laser generation at 193 nm by frequency mixing in LBO crystals

Zhitao Zhang,[a] Hanghang Yu,[a] Sheng Chen,[a] Zheng Li,[a] Xiaobo Heng,[a] and Hongwen Xuan[a,b,*]
[a]Chinese Academy of Sciences, GBA branch of Aerospace Information Research Institute, Guangzhou, China
[b]University of Chinese Academy of Sciences, Beijing, China

Abstract. A 60-mW solid-state deep ultraviolet (DUV) laser at 193 nm with narrow linewidth is obtained with two stages of sum frequency generation in LBO crystals. The pump lasers, at 258 and 1553 nm, are derived from a homemade Yb-hybrid laser employing fourth-harmonic generation and Er-doped fiber laser, respectively. The Yb-hybrid laser, finally, is power scaling by a 2 mm × 2 mm × 30 mm Yb:YAG bulk crystal. Accompanied by the generated 220-mW DUV laser at 221 nm, the 193-nm laser delivers an average power of 60 mW with a pulse duration of 4.6 ns, a repetition rate of 6 kHz, and a linewidth of ∼640 MHz. To the best of our knowledge, this is the highest power of 193- and 221-nm laser generated by an LBO crystal ever reported as well as the narrowest linewidth of 193-nm laser by it. Remarkably, the conversion efficiency reaches 27% for 221 to 193 nm and 3% for 258 to 193 nm, which are the highest efficiency values reported to date. We demonstrate the huge potential of LBO crystals for producing hundreds of milliwatt or even watt level 193-nm laser, which also paves a brand-new way to generate other DUV laser wavelengths.

Keywords: 193 nm; solid-state laser; deep ultraviolet; LBO crystal; sum frequency mixing; narrow linewidth.

1 Introduction

Coherent light sources at the deep ultraviolet (DUV) region are important to the applications of lithography, defect inspection, metrology, and spectroscopy.[1–3] For example, a high-power 193-nm laser has been successfully applied in lithography as a system consisting of an ArF oscillator and an amplifier. However, the poor coherence of ArF excimer laser, originating from the principle of the excimer laser, limits the possibility for applications, such as interference lithography demanding high-resolution patterns. By replacing the ArF oscillator with a narrow linewidth solid-state 193-nm laser seed, both narrow linewidth and high coherence could be achieved for the DUV laser at 193 nm, which is so-called "hybrid ArF excimer laser."[4] It will be beneficial for high-throughput inference lithography in terms of pattern precision and lithography speed.[5] Moreover, the high photon energy and high coherence of the hybrid ArF excimer

laser enables it to directly process various carbon compounds and solid materials without significant thermal effect.[6] It can be seen from the above that a solid-state 193-nm laser seed with narrow linewidth and good beam quality could not only improve coherence but also maintain the high output power of the hybrid ArF excimer laser system, benefiting both interference lithography and laser machining. Hence, to optimally seed an ArF amplifier, the linewidth at full width at half-maximum (FWHM) of the 193-nm seed laser should be <4 GHz (FWHM < 0.5 pm),[4,7] which will determine the coherence length of interference and is easier to obtain via using solid-state laser technologies. Consequently, the generation of 193 nm based on solid-state lasers has attracted increased research interest in the past decades, as well as for the purpose of semiconductor inspection and metrology.

The common way to build a DUV source based on solid-state laser is through multistage frequency conversion from the near-infrared, with solid or fiber lasers as pump sources. First, the advancement of high-power solid-state lasers, such as thin-disk

---

lasers, single-crystal fiber (SCF) lasers, Ti:sapphire lasers, and fiber lasers, enables the pump sources to compensate for the energy loss during frequency conversion processes and obtain bright DUV light.[8–11] Recent advancements have shown the bulk crystal can achieve comparable performance to the SCF scheme in power amplification, which will further reduce the expense of the DUV laser system.[12] Second, while the generation of continuous-wave 193 nm light often requires the addition of an enhancement cavity to obtain a higher conversion efficiency,[10,13] pulsed laser generation benefits from the associated higher peak power and can be more straightforwardly implemented. Numerous variations of such multistage architecture have been demonstrated for pulsed 193 nm generation in the past decades, with increasing output power reported. In 2003, Kawai et al. realized an average power of 140 mW light source at 193 nm with a repetition rate of 200 kHz, by eighth-harmonic generation from a pulsed Er-doped fiber at 1547 nm.[14] In 2015, Tsuboi et al. realized the output power of 230 mW at 193 nm by mixing the fourth harmonic of the 904 nm Ti:sapphire laser with a 1342 nm Nd:YVO$_4$ laser.[15] In the same year, Xuan et al. demonstrated a 300-mW pulsed solid laser at 193 nm with repetition rate of 6 kHz, based on frequency mixing between a 1553 nm fiber laser and a 258 nm laser that conversed from a 1030 nm Yb-hybrid laser via fourth harmonic generation (FHG).[16] Later, they developed the system with a 10 kHz repetition rate to output more than 1 W at 193 nm.[17] Although, in all these demonstrations of solid-state 193-nm pulsed laser, it could achieve a high power of more than 100 mW, the narrowest reported linewidth so far has been 4 GHz, which can be improved upon.

Aside from the pump laser, the choice of nonlinear optical crystal is also important for improving the reliability, ease of use, and the lowering of costs for wider adoption in the industry. Three of the most popular nonlinear optical crystals for DUV generation are BaB$_2$O$_4$ (BBO), LiB$_3$O$_5$ (LBO), and CsLiB$_6$O$_{10}$ (CLBO) crystals.[17–20] Several of their significant characteristics are summarized in Table 1. The BBO crystal has an obviously high nonlinear coefficient and damage threshold, which allows it to tolerate strong pump lasers and generate high-power DUV light easily. However, the big walk-off angle of BBO crystals induces degradation to the beam quality of the generated DUV light. What is more, BBO has a strong absorption at 193 nm, which limits the output power and introduces thermal effects, such as thermal-induced dephasing, that can degrade long-term operation.[21] And therefore, crystal cooling is needed to achieve high power and optimal stability. As an alternative, the CLBO crystal has been widely used in recent DUV generation systems and provides a high average power of up to 1 W at 193 nm and a conversion efficiency of more than 47%.[17] The wide phase-matching (PM) range enables various

sum frequency generation (SFG) of type-I and type-II phase matching in CLBO crystals. Although CLBO may be the best nonlinear crystal for high-power DUV laser generation in terms of the trade-off between high power and good beam quality, the hygroscopic deterioration necessitates the CLBO crystal to be housed in a dry clean air environment and heated to more than 150°C, which adds to the complexity.[22,23] It is still cost-prohibitive, especially for large-dimension crystal (e.g., 100 mm × 100 mm × 100 mm), hindering the development of affordable, high-power 193-nm laser systems.[24] Power scaling up while maintaining cost-effectiveness is yet a challenge for 193-nm laser using CLBO.

On the other hand, LBO[25–27] can readily adapt to standard laboratory environments and is several times cheaper than CLBO in cost. Although the nonlinear coefficient d_{eff}, of 0.254 at 193 nm is much lower compared with the 0.992 of CLBO, as shown in Table 1, this could be compensated for with a longer crystal due to the smallest walk-off angle and wide angular acceptance of LBO.[28] Reduced complexity and lower costs make LBO an excellent candidate for 193-nm lasers in industrial applications.

In this paper, we demonstrate a narrow linewidth, nanosecond-pulsed laser at 193 nm based on two stages of cascaded SFG in LBO crystals. The pump light is generated from two actively synchronized pulsed lasers operating at 1030 and 1553 nm, respectively. The maximum output power at 193 and 221 nm is 60 and 220 mW, respectively. To the best of our knowledge, it is the highest average power ever reported for both 193- and 221-nm lasers by frequency mixing in LBO crystals. The conversion efficiency is 27% for 221 to 193 nm and 3% for 258 to 193 nm, which is the highest conversion efficiency ever reported using LBO. The 193-nm laser has a pulse duration of 4.6 ns and a repetition rate of 6 kHz, corresponding to a pulse energy of 10 μJ. The linewidth of a 193-nm laser is estimated to be <640 MHz (<0.08 pm), which is the narrowest one from a solid-state pulsed laser using LBO crystal so far. These remarkable results confirm the viability of pumping LBO with solid-state lasers for reliable and effective generation of a narrow linewidth laser at 193 nm and unblock a new way to fabricate a cost-effective, high-power DUV laser system using LBO.

2 Experimental Setup

The overview of the experimental setup is shown in Fig. 1. Two synchronized homemade pulsed lasers operating at 1030 and 1553 nm are used as the fundamental sources. The 258-nm laser, produced from the FHG of the 1030-nm laser, serves as the pump light which, together with the 1553 nm light, generates the 193 nm in two cascaded SFG processes in the LBO crystal.

The experimental scheme of the pulsed 1030-nm Yb-hybrid laser is shown in Fig. 2. A narrow linewidth (<10 kHz) continuous-wave fiber laser at 1030 nm with 100 mW output power is intensity-modulated by an acoustic-optics modulator (AOM) to produce a pulse train of 96-kHz repetition rate and 15-ns pulse duration. To compensate for the power loss induced by the first AOM, the 0.3 mW pulsed laser light is preamplified to 30 mW by a single-mode fiber preamplifier and has its repetition rate decreased to 6 kHz via the second AOM, matching the repetition rate of the commercially available ArF excimer laser system. The timing signals of the two AOMs are synchronized by a digital delayer (DG645, Stanford Research Systems). The 6-kHz pulse train is amplified by another single-mode fiber

Table 1 Optical properties of BBO, CLBO, and LBO at 193 nm (1553.3 + 220.9 nm->193.4 nm, type I).

	Walk-off angle (mrad)	d_{eff} (pm/V)	Angular acceptance (mrad·cm)
BBO	110.60	2.400	0.10
CLBO	38.95	0.992	0.32
LBO	10.87	0.254	1.05
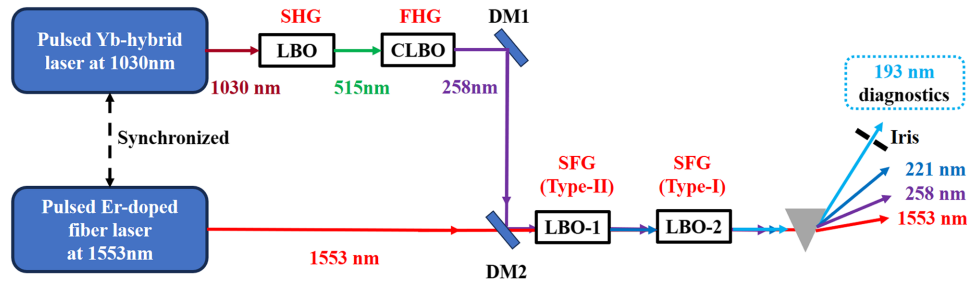
Fig. 1 Experimental setup of the 193-nm laser system. SHG, second-harmonic generation; FHG, fourth-harmonic generation; SFG, sum frequency generation; DM1, AR@515 nm/HR@258 nm dichroic mirror; DM2: HR@258 nm/AR@1553 nm dichroic mirror.
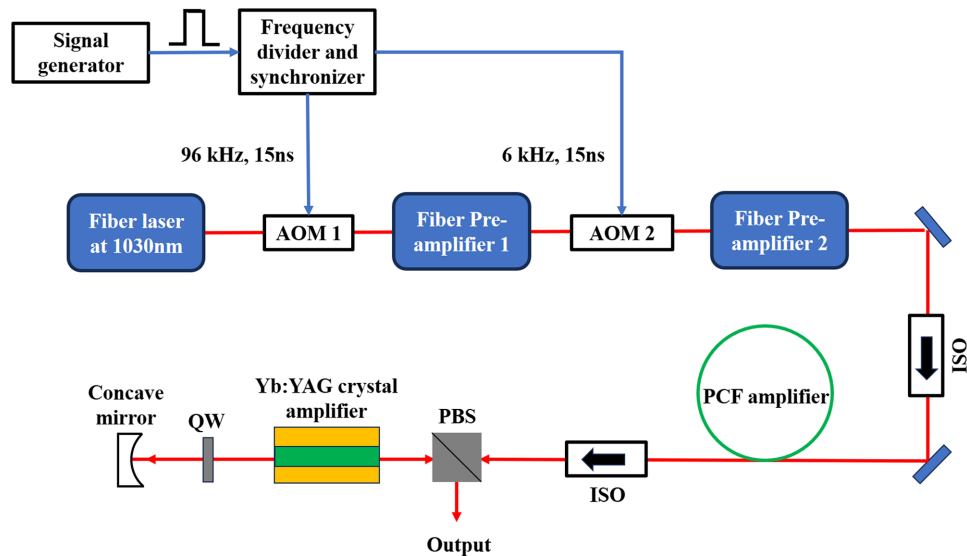
Fig. 2 Experimental setup of the 1030 nm Yb-hybrid pulsed laser. AOM, acoustic-optics modulator; ISO, isolator; PCF, photonic crystal fiber; PBS, polarization beam splitter; QW, quarter-wave plate.

preamplifier from 1 to 10 mW, to seed a 90 cm-long Yb-doped photonic crystal fiber (PCF) amplifier pumped by a 14 W multimode laser diode (LD) at 976 nm. With the boosted 800-mW laser power from the PCF amplifier, a Yb:YAG bulk crystal (atomic fraction of 2%, 2 mm × 2 mm × 30 mm) is inserted to be the final-stage main amplifier. The Yb:YAG bulk crystal is mounted in a water-cooled copper heat sink with the temperature regulated at 16°C and end-pumped by a 100 W multimode LD at 969 nm. The Yb:YAG bulk amplifier is built in a double-pass configuration to improve the gain and output power.

The 1553-nm laser constituting the other pillar for the SFG process is also developed in-house. A commercial continuous-wave DFB laser operating at the wavelength of 1553.3 nm with 12 mW output power is optically switched by a semiconductor optical amplifier. The generated pulsed laser is then amplified by three stages of Er-doped fiber amplifiers, and its output power reaches 600 mW with a pulse duration of 10 ns and linewidth of <400 MHz. Note that the switch signal of the semiconductor optical amplifier is also provided by the same DG645, ensuring that the pulse train is synchronized with that of the 258 nm laser. More details of this 1553 nm fiber laser system can be found in our previous paper.[29]

3 Results and Discussion

For the 1030 nm fundamental source, compared with the single-pass configuration, the double-pass configuration has an evident improvement in output power region, as shown in Fig. 3(a). The output power grows linearly as the pump power of 969 nm increases and shows no sign of saturation. With the double-pass configuration, the SCF amplifier provides a gain of nearly 8 and output power of 14.6 W with 100 W of pump light. The beam profiles of the 1030-nm laser output from the Yb:YAG bulk amplifier along propagation behind a lens of 200 mm focal length are measured via a CCD camera, as shown in Fig. 3(b). With Gaussian fitting, the beam quality factor M^2 in horizontal and vertical axes is calculated to be ∼1.08 and 1.12, respectively. There are hardly any distortions to the excellent spot roundness, implying minimal thermal degradation in the Yb:YAG bulk.[30] The pulse duration of the 14.6 W output is measured to be 13.1 ns, and the linewidth is <150 MHz measured by a scanning Fabry–Perot interferometer.

For the ArF hybrid excimer laser, the SCF scheme offers advantages over the other schemes as the seed amplifier.[4] Its compactness, including pumping with an LD, fits the dimension

(a)

(b)
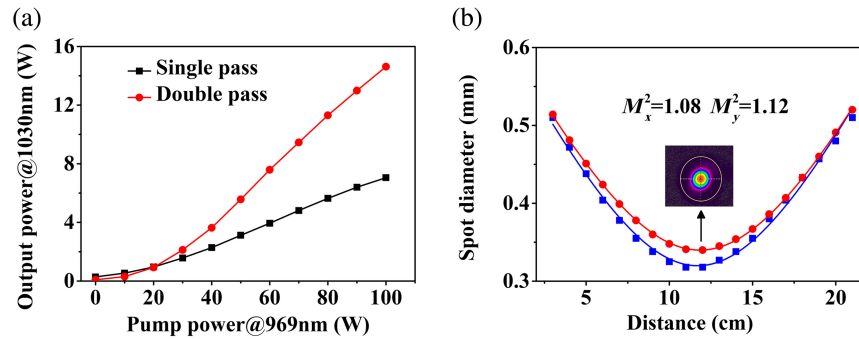
Fig. 3 (a) Output power versus pump power in the Yb:YAG bulk crystal amplifier with single-pass and double-pass configurations; (b) the beam profiles of the 1030-nm laser output at 14.6 W of Yb:YAG bulk crystal.

constraint of the traditional "twin chamber" or "chamber dual" ArF excimer laser system. Furthermore, it is more convenient and efficient for narrow linewidth laser amplification compared with fiber lasers in terms of exhibiting a higher stimulated Brillouin scattering threshold. Here, we demonstrate that the Yb:YAG bulk has exactly the same amplifier performance compared to that of SCF,[5,16,17] showing the potential of leading to a more cost-effective DUV laser system.

With the pulsed laser of average power of 14.6 W at 1030 nm, 515 nm green light is produced by second-harmonic generation (SHG) within an LBO crystal (CASTECH) using a noncritical phase-matching (NCPM) scheme. The size of the LBO crystal is 5 mm × 5 mm × 30 mm and it has an anti-reflection (AR) coating for 1030 and 515 nm on both ends. To meet the NCPM condition of the LBO, the crystal is held in a copper holder and heated to 185°C. Launching the 1030 nm beam with a diameter of 340 μm, corresponding to a power density of nearly 200 MW/cm², the maximum generated output power and conversion efficiency for the 515 nm light reach nearly 10 W and 70%, respectively, as shown in Fig. 4(a). The generated 515 nm green light, with a pulse duration of ~10 ns, is separated from the 1030-nm light with two dichroic mirrors, with a high-reflection (HR) coating @ 515 nm and an AR coating @ 1030 nm. As there is no phase-matched angle in LBO crystal to generate 258 nm laser, BBO and CLBO become the two alternatives for FHG. Since the walk-off angle of BBO is 3 times larger than that of CLBO, a piece of CLBO crystal (5 mm × 5 mm × 19 mm, θ = 66.2 deg, φ = 45.0 deg, critical PM, CASTECH) is chosen for FHG. The CLBO crystal is placed in the Ar gas environment and heated to more than

150°C to prevent the hydroscopic reaction problem. To avoid laser-induced damage, both the input and output ends of the crystal are polished, while only the input end has an AR coating @ 515 nm. As shown in Fig. 4(b), the output highest average power of 258-nm laser is 2 W, corresponding to a conversion efficiency of only 20%, which is lower than that in previous reports.[16,17,31] Actually, we could also obtain 30% − 40% conversion efficiency at this stage in our setup. However, to protect the coating of the dichroic mirror DM1 (shown in Fig. 1), the highest power density of the 515 nm laser in the CLBO crystal is limited to about 50 MW/cm², which is also an optimization, as well as to mitigate the power degradation, commonly occurring in the nonlinear crystals.[32] In other words, it is a trade-off between conversion efficiency and long-term operation. In addition, this trade-off will further benefit the conversion efficiency of the final SFG stage of the 193-nm laser.

As shown in Fig. 1, to generate the 193-nm laser, a 221-nm laser is first generated by SFG between the 258- and 1553-nm laser. Then, the 221- and the residual 1553-nm light exhibit the second SFG to output the final 193-nm laser. Normally, the two stages of SFG are separated, meaning the need for two specialized assemblies for each pump laser, which increases the complexity and cost of the system. To simplify the setup, the collinear cascaded scheme is introduced in our work including type-I and type-II PM schemes.[19] For the first SFG, the LBO-1 crystal (5 mm × 5 mm × 20 mm, θ = 55.6 deg, φ = 90 deg, CASTECH) is chosen to generate a 221-nm laser, under type-II PM [1553 nm(o) + 258 nm(e) → 221 nm(o)]. For the second SFG, the LBO-2 crystal (5 mm × 5 mm × 20 mm, θ = 90 deg, φ = 76.4 deg, CASTECH) is chosen to generate the 193-nm

(a)

(b)
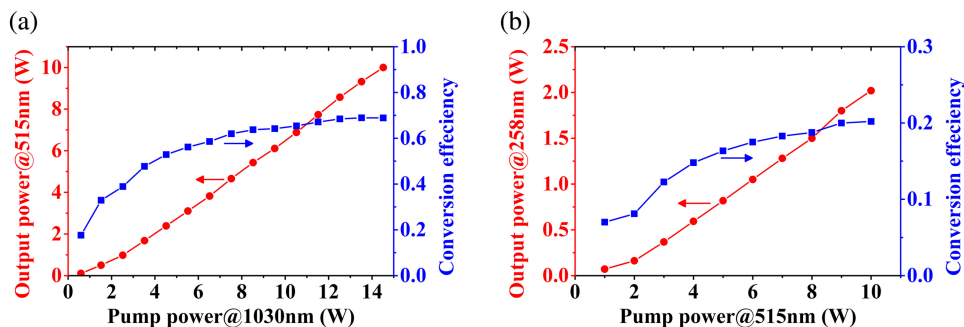
Fig. 4 Output average powers of (a) 515-nm laser and (b) 258-nm laser as the function of pump average powers of 1030 and 515 nm lasers, respectively.

laser, under type-I PM [1553 nm(o) + 221 nm(o) → 193 nm(e)]. The polarization of the 221 nm and the residual 1553 nm laser output from the first SFG satisfies the type-I PM condition of the second SFG. Consequently, two LBO crystals could be placed in tandem without additional polarization adjustments. Moreover, it is worth noting that the pulse trains of the 221 and the 1553 nm laser are also synchronized automatically in the second LBO crystal. To optimize the pump condition of the cascaded SFG process, the pump lasers should propagate with an adequately long Rayleigh length covering the two LBO crystals. This sets a minimum size for the focus spot and constrains the achievable power density. The spot waist diameters of the 258- and 1553-nm laser beams are regulated to 500 and 400 μm, respectively, and the two beams are combined with dichroic mirror DM2. Before inserting the LBO-2 crystal, the 221-nm laser generated from the LBO-1 crystal is separated by a calcium fluoride (CaF$_2$) prism for diagnostics. With the 1553-nm pump power at 600 mW, a maximum output power of 220 mW but conversion efficiency only of 10.9% at 221 nm is obtained, lower than that of more than 20% at a low pump, as shown in Fig. 5(a). Two factors contribute to the efficiency reduction in this SFG stage: first, the focus power intensity of 258-nm laser is not optimized for 221-nm laser generation; second, the high-power pump laser beams' size may change due to the thermal effect.[9] Interestingly, after inserting the LBO-2 crystal following the LBO-1 for the second SFG stage, a laser power of 60 mW at 193 nm is generated corresponding to a conversion efficiency of 27%, as shown in Fig. 5(b). Hence, the total efficiency is ~3% for 258 to 193 nm. To date, 27% for 221 to 193 nm and 3% for 258 to

193 nm is the highest conversion efficiency ever reported using an LBO crystal.

According to the linewidth of 1030 nm (~150 MHz) and 1553 nm laser (~400 MHz), the linewidth of the 193-nm laser is estimated to be ~640 MHz, corresponding to an FWHM < 0.08 pm. The pulse energy is 10 μJ according to the repetition rate of 6 kHz. The pulse duration of the 193-nm laser is measured to be ~4.6 ns using a biplanar phototube, as shown in Fig. 6. The short pulse duration may result from the frequency uncertainty of the pump laser that would be transferred and even increased during the nonlinear frequency conversion, which leads to the linewidth broadening and pulse narrowing of the 193-nm laser. The inset in Fig. 6 shows the beam profile with an optical diameter of ~1 mm of the 193-nm laser in the far field measured by a pyroelectricity camera (Ophir Pyrocam III HR). Due to the small walk-off angle in LBO crystals, the 193 nm laser inherits excellent beam quality from the pump lasers. To measure the beam quality of the UV/DUV laser, a scanning-slit beam profiler (NS2s-PYRO/9/5-STD, Ophir) is employed to record the beam diameter variation along the propagation direction, with minimum measurable beam of 7 μm, overcoming the resolution limitations of the pyroelectricity camera. Using the beam profiler, the laser beam quality M^2 of 258 nm is measured to be 1.24 and 1.18 in vertical and horizon directions, respectively, while the 221-nm laser obtained M^2 values of 1.29 and 1.21. Due to the limited sensitivity of the scanning-slit beam profiler, it is feasible to directly measure the beam quality of the generated 193-nm laser. However, since the SFG for the 193-nm laser is cascaded with that of the 221-nm laser and pumped by the 221-nm laser, it could be inferred that
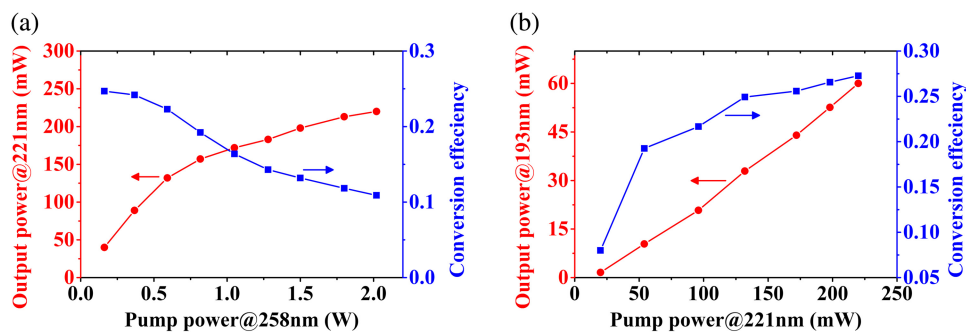
Fig. 5 Output average powers of (a) 221-nm laser and (b) 193-nm laser generated from the first and second SFG in LBO crystal as a function of pump average powers of 258 and 221 nm lasers, respectively.
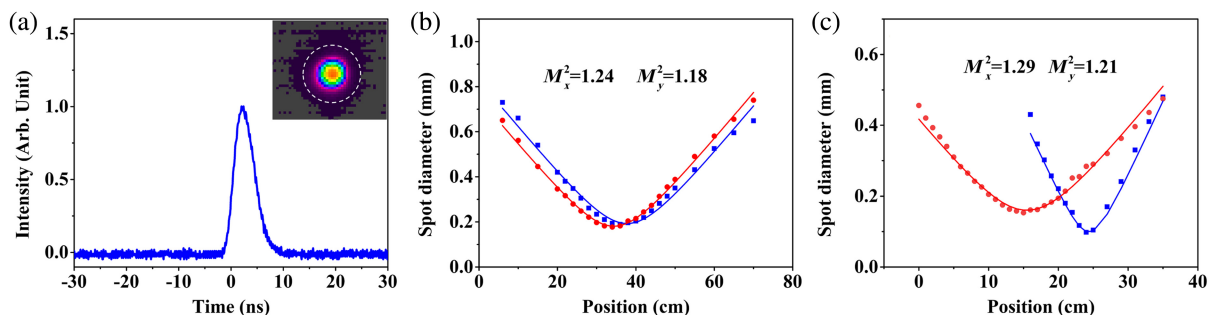
Fig. 6 (a) Pulse duration of the generated 193 nm laser. Inset: Beam profile of the 193-nm laser. Measured beam profiles of (b) the 258-nm laser and (c) the 221-nm laser.
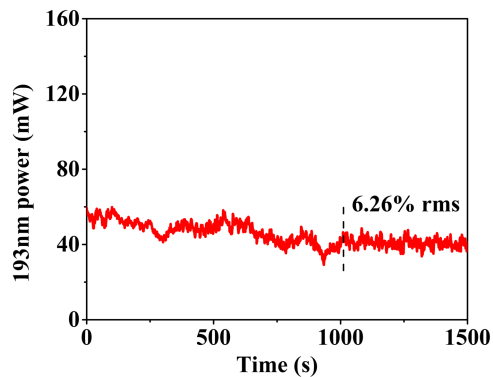
Fig. 7 Power stability of the free-running 193-nm laser within 1500 s.

the 193-nm laser has almost an identical beam quality with the 221-nm laser.

The power stability of the 193-nm laser within 1500 s is shown in Fig. 7. During the first 1000 s, the output power has an obvious fluctuation and gradually degrades from 60 to nearly 40 mW. The fluctuation comes from the free-running pump lasers, as they operate without any power-locking scheme. Moreover, the LBO crystals for generating 221- and 193-nm lasers are mounted on clamps without any temperature control. The increased heat induced by the pump lasers brings the phase mismatching within the crystals, leading to severe power fluctuations. Therefore, when the crystals reach the heat balance, the 193-nm laser shows a more stable characteristic during the last 500 s, with an average power of 40 mW and stability of 6.26% rms. It is worth noting that the power would recover to 60 mW by finely adjusting the angle of the LBO crystal, which proves that power fluctuation results from phase mismatch in turn. We believe that the 193 nm laser could present a more optimistic behavior if the temperature controller for LBO crystals and power-locking systems are introduced.

4 Conclusion

We demonstrated a high-power, narrow linewidth 193-nm pulsed laser by cascaded frequency mixing in LBO crystals between an Er-doped fiber laser and a Yb-hybrid laser. A maximum average power of 60 mW at 193 nm with a 4.6 ns pulse duration is obtained at a repetition rate of 6 kHz, while maximum average power of 220 mW at 221 nm is also achieved. The conversion efficiency is 27% for 221 to 193 nm and 3% for 258 to 193 nm. To the best of our knowledge, it not only achieves the highest average power ever reported for both 193- and 221-nm lasers by SFG using an LBO crystal but also demonstrated the highest DUV conversion efficiency recorded by an LBO. The 193-nm laser has a linewidth of ~640 MHz, which is the narrowest obtained so far using frequency mixing in LBO, and a nearly circular beam profile in the far field. The output is suitable for seeding ArF excimer amplifiers to generate highly coherent DUV for lithography. In addition, although the LBO has a smaller nonlinear coefficient in the DUV region compared to others, it could be grown and cut to an impressive large dimension[33] while still maintaining a low cost, which allows for compensation through a longer interaction length. This paves a new way for further power scaling up of a cost-effective DUV laser system by the use of LBO crystals in the future.

Disclosures

The authors declare no conflicts of interest.

Code and Data Availability

Data underlying the results presented in this paper are not publicly available at this time but may be obtained from the authors upon reasonable request.

References

1. M. Totzeck et al., "Pushing deep ultraviolet lithography to its limits," *Nat. Photonics* **1**(11), 629–631 (2007).
2. B. M. Barnes et al., "Three-dimensional deep sub-wavelength defect detection using $\lambda = 193$ nm optical microscopy," *Opt. Express* **21**(22), 26219–26226 (2013).
3. A. D. Shutov et al., "Highly efficient tunable picosecond deep ultraviolet laser system for Raman spectroscopy," *Opt. Lett.* **44**(23), 5760–5763 (2013).
4. S. Tanaka et al., "Development of high coherence high power 193 nm laser," *Proc. SPIE* **9726**, 972624 (2016).
5. B. Päivänranta et al., "Sub-10 nm patterning using EUV interference lithography," *Nanotechnology* **22**(37), 375302 (2011).
6. M. Kobayashi et al., "DUV high power lasers processing for glass and CFRP," *Proc. SPIE* **10238**, 102381D (2017).
7. H. Xuan et al., "Development of narrow-linewidth Yb- and Er-fiber lasers and frequency mixing for ArF excimer laser seeding," *Proc. SPIE* **8961**, 89612M (2014).
8. J. Zhang et al., "Distributed Kerr lens mode-locked Yb:YAG thin-disk oscillator," *Ultrafast Sci.* **2022**, 9837892 (2022).
9. H. Xuan et al., "High-power and high-conversion efficiency deep ultraviolet (DUV) laser at 258 nm generation in the $CsLiB_6O_{10}$ (CLBO) crystal with a beam quality of $M^2 < 1.5$," *Opt. Lett.* **42**(16), 3133–3136 (2017).
10. J. Sakuma et al., "Continuous-wave 193.4 nm laser with 120 mW output power," *Opt. Lett.* **40**(23), 5590–5593 (2015).
11. M. Müller et al., "High-average-power femtosecond laser at 258 nm," *Opt. Lett.* **42**(14), 2826–2829 (2017).
12. A. M. Rodin et al., "Comparison of Yb:YAG single crystal fiber with larger aperture CPA pumped at 940 nm and 969 nm," in *Conf. on Lasers and Electro-Opt. Pac. Rim*, Optica Publishing Group, p. s1905 (2017).
13. M. Scholz et al., "A bright continuous-wave laser source at 193 nm," *Appl. Phys. Lett.* **103**(5), 051114 (2013).
14. H. Kawai et al., "UV light source using fiber amplifier and non-linear wavelength conversion," in *Conf. Lasers and Electro-Opt.*, Optica Publishing Group, p. CTuT4 (2003).
15. M. Tsuboi et al., "Development of high-power, 6 kHz, single-mode Ti: sapphire laser at 904 nm for generating 193 nm light," *Jpn. J. Appl. Phys.* **54**(4), 042702 (2015).
16. H. Xuan et al., "300-mW narrow-linewidth deep-ultraviolet light generation at 193 nm by frequency mixing between Yb-hybrid and Er-fiber lasers," *Opt. Express* **23**(8), 10564–10572 (2015).
17. H. Xuan et al., "1 W solid-state 193 nm coherent light by sum-frequency generation," *Opt. Express* **25**(23), 29172–29179 (2017).
18. Z. Zhao et al., "Watt-level 193 nm source generation based on compact collinear cascaded sum frequency mixing configuration," *Opt. Express* **26**(15), 19435–19444 (2018).

19. D. G. Nikitin et al., "Sum frequency generation of UV laser radiation at 266 nm in LBO crystal," *Opt. Lett.* **41**(7) 1660–1663 (2016).
20. Q. Fu et al., "High-power, high-efficiency, all-fiberized-laser-pumped, 260-nm, deep-UV laser for bacterial deactivation," *Opt. Express* **29**(26), 42485–42494 (2021).
21. A. J. Merriam et al., "Efficient nonlinear frequency conversion to 193-nm using cooled BBO," in *Adv. Solid-State Photonics*, Optica Publishing Group, p. MB11 (2007).
22. K. Kohno et al., "High-power DUV picosecond pulse laser with a gain-switched-LD-seeded MOPA and large CLBO crystal," *Opt. Lett.* **45**(8), 2351–2354 (2020).
23. T. Kawamura et al., "Effect of water impurity in $CsLiB_6O_{10}$ crystals on bulk laser-induced damage threshold and transmittance in the ultraviolet region," *Appl. Opt.* **48**(9), 1658–1662 (2009).
24. X. Yuan et al., "Growth and characterization of large CLBO crystals," *J. Cryst. Growth* **293**(1), 97–101 (2006).
25. R. D. Mead, C. E. Hamilton, and D. D. Lowenthal, "Solid state lasers for 193-nm photolithography," *Proc. SPIE* **3051**, 882–889 (1997).
26. C. E. Hamilton et al., "All solid-state, single-frequency 193-nm laser system for deep-UV metrology," in *Conf. Proc. LEOS'98. 11th Annu. Meet. IEEE Lasers and Electro-Opt. Soc. 1998 Annu. Meet. (Cat. No. 98CH36243)*, IEEE, Vol. 1, pp. 322–323 (1998).
27. T. Ohtsuki et al., "193-nm generation by eighth harmonics of Er^{3+}-doped fiber amplifier," in *Conf. Lasers and Electro-Opt.*, Optica Publishing Group, p. PD9 (2000).
28. A. Borsutzky, R. Brünger, and R. Wallenstein, "Tunable UV radiation at short wavelengths (188–240 nm) generated by sum-frequency mixing in lithium borate," *Appl. Phys. B* **52**, 380–384 (1991).
29. Z. Zhang et al., "10 kW peak power, single-frequency 1553 nm nanosecond pulsed fiber laser for time-of-flight LIDAR," *Appl. Phys. Express* **16**(2), 022002 (2013).
30. Y. Zaouter et al., "Direct amplification of ultrashort pulses in μ-pulling-down Yb: YAG single crystal fibers," *Opt. Lett.* **36**(5), 748–750 (2011).
31. Y. Orii et al., "Stable 10,000-hour operation of 20-W deep ultraviolet laser generation at 266 nm," *Opt. Express* **30**(7), 11797–11808 (2022).
32. K. Takachiho et al., "Ultraviolet laser-induced degradation of $CsLiB_6O_{10}$ and β-BaB_2O_4," *Opt. Mater. Express* **4**(3), 559–567 (2014).
33. Z. Hu, "Development of large-size LBO crystal growth," in *JSAP-OSA Joint Symp.*, Optica Publishing Group, p. 18a_D5_4 (2013).

Biographies of the authors are not available.